Design and Analysis of Wave Sensing Scheduling Protocols for Object-Tracking Applications

Shansi Ren, Qun Li, Haining Wang, and Xiaodong Zhang

College of William and Mary,
Williamsburg, VA 23187 USA
{sren, liqun, hnw, zhang}@cs.wm.edu

Abstract. Many sensor network applications demand tightly-bounded object detection quality. To meet such stringent requirements, we develop three sensing scheduling protocols to guarantee worst-case detection quality in a sensor network while reducing sensing power consumption. Our protocols emulate a line sweeping through all points in the sensing field periodically. Nodes wake up when the sweeping line comes close, and then go to sleep when the line moves forward. In this way, any object can be detected within a certain period. We prove the correctness of the protocols and evaluate their performances by theoretical analyses and simulation.

1 Introduction

Detecting and tracking moving objects is a major class of applications in sensor networks. Many of these applications demand stringent object detection quality. A simple solution to meeting required object detection quality is full sensing coverage, in which intruding objects can be timely detected . However, full sensing coverage requires that a large portion of the sensors remain awake continuously, resulting in energy inefficiency and short system lifetime. As an alternative approach, probabilistic sensing coverage has been recently proposed in [5, 12]. Instead of staying awake all the time, nodes can periodically rotate between active state and sleeping state to conserve energy while meeting the object detection quality requirement. Compared with full sensing coverage, probabilistic sensing coverage leads to significant energy conservation and much longer system lifetime.

The previous work on probabilistic coverage focused on providing average-case object detection quality for surveillance applications. Thus far, little attention in the literature has been paid to designing protocols that guarantee bounded worst-case object detection quality. Many military surveillance applications, however, often demand such stringent object detection quality requirements, e.g., an enemy vehicle must be detected in one minute. To address this problem, we propose wave sensing, a new sensing scheduling scheme under probabilistic coverage to provide bounded worst-case object detection quality. In this scheme, at any moment, active nodes on the sensing field form connected curves. These curves move back and forth both horizontally and vertically across the field, so that every geographical point is scanned at least once within a limited amount of time. In this way, the wave sensing scheme can guarantee that an object

V. Prasanna et al. (Eds.): DCOSS 2005, LNCS 3560, pp. 228–243, 2005.

is detected with certainty (i.e., 100% probability) in a given observation duration, and the distance it traversed before detection is bounded.

Specifically, we develop three wave sensing schedules to provide guaranteed worst-case object detection quality in terms of sufficient phase and worst-case stealth distance[1]. We prove several properties of these schedules, and mathematically analyze their average-case object detection quality. We also investigate energy consumption of the wave protocols. Our protocol design and analyses provide insights into the interactions between object detection quality, system parameters, and network energy consumption. Given a worst-case object detection quality requirement, we are able to optimize average-case object detection quality as well as network energy consumption by choosing appropriate network parameters. We evaluate the performance of the wave protocols through extensive simulation experiments.

The rest of the paper is organized as follows. We formulate the object detection and tracking problem in Section 2. Three wave sensing scheduling protocols are presented and analyzed in Section 3. In Section 4, we investigate average-case object detection quality of the protocols under a model for wave sensing protocols. We evaluate the performance of the protocols in Section 5. Section 6 sketches related work. Finally, we conclude our work in Section

2 Object Detection and Tracking Problem Formulation

We assume that sensors are randomly and independently deployed on a square sensing field. The field can be completely covered when all nodes are active. Considering the vastness of the sensing field, the size of a moving object is negligible. In a sensing schedule, a node periodically wakes up and goes to sleep to conserve energy.

We define two metrics to characterize average object detection quality:

- *Detection Probability* (DP). The detection probability is defined as the probability that an object is detected in a given observation duration.
- *Average Stealth Distance* (ASD). The average stealth distance is defined as the average distance an object travels before it is detected for the first time.

For worst-case object detection quality of the network, we have the following two metrics:

- *Sufficient Phase* (SP). The sufficient phase is defined as the smallest time duration in which an object is detected with certainty no matter where the object initially appears on the field.
- *Worst-case Stealth Distance* (WSD). The worst-case stealth distance is defined as the longest possible distance that an object travels before it is detected for the first time.

Taking energy constraints into account, we further define the following metric:

- *Lifetime*. The system lifetime is the elapsed working time from system startup to the time when the object detection quality requirement cannot be met for the first time, with the condition that live nodes continue their current sensing periods.

[1] Sufficient phase and worst-case stealth distance are formally defined in Section 2.

In our previous protocol design of the random and the synchronized schedules in [12], we focused on how to meet the requirements of detection probability, average stealth distance and energy consumption. However, worst-case object detection quality metrics, such as sufficient phase and worst-case stealth distance, are not bounded in these protocols. Given an observation duration, an object can escape the detection; it can also travel an infinite distance even its average stealth distance is small. In practice, many applications demand stringent requirements on worst-case object detection quality. For example, an object must be detected in 10 seconds with certainty. Therefore, we aim to design sensing scheduling protocols that achieve a bounded sufficient phase and worst-case stealth distance, while minimizing energy consumption of the system.

3 Design of Wave Sensing Protocols

In this section, we present three wave sensing protocols. The main idea behind these protocols is as follows. When the distance between any two nodes is less than their sensing diameter $2R$, their sensing ranges intersect and form a connected region. If currently-active nodes make up a connected stripe with two ends on opposite borders of the field, the stripe divides the field into two halves. Under such a circumstance, in a sufficiently long time duration, an object can be detected when it crosses this stripe. For any specified continuous curve with two ends on opposite borders of the field, it is always possible to find a set of nodes whose sensing ranges completely cover this curve under the assumption that the field are completely covered when all nodes wake up. To further reduce the detecting time, we allow the curve to move so that every geographical point on the field can be scanned at least once, without leaving any sensing hole in a limited amount of time. We define the curve (line) to be covered as the *active curve (line)*, and define the union of the sensing ranges of all active sensors that cover the active curve (line) as the *hot region*.

We aim to design protocols that ensure: 1) the hot region should have no sensing hole in it; 2) the hot region should be as thin as possible in order to save the network energy consumption; 3) the active curve should move circularly like sea waves, so that the object can be detected rapidly and energy consumption variance among nodes is small.

3.1 Line Wave Protocol Design

In this protocol, we make two assumptions. First, we assume that every node on the field has a timer that is well synchronized with others. The global timer synchronization techniques of [8] can be used in this protocol. Second, we assume that every node is aware of its own geographical location on the field through some method, either by GPS or some other localization techniques.

Line Wave Protocol Description. In the line wave protocol, the active curve is a straight line, as shown in Fig. 1. This protocol is specified as follows.

1. At the system startup time, all nodes synchronize their timers, and obtain their geographical coordinates. There are two active lines on the two opposite borders of the field moving towards the center. All nodes are informed of the initial positions,

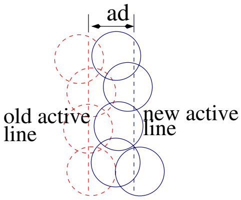

Fig. 1. Line wave protocol illustration

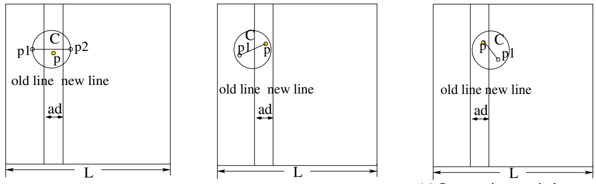

(a) All points in C are between two lines.

(b) Some points are in between, some are on left of old line.

(c) Some points are in between, some are on right of new line.

Fig. 2. There is no sensing hole in hot regions of the line wave protocol

the settling time, and the advancing distance (ad) of the active lines. Note that $ad < 2R$.

2. Every node computes current positions of the active lines based on its timer and the information of the active lines it obtained. Then, it calculates if its sensing range intersects the active lines. If there is intersection, this node wakes up.
3. After the active lines have stayed at their current positions for their settling time, they move forward with a distance ad towards the field center. When they reach the center, they go back to the field borders. Step 2 repeats.

Note that a sleeping node periodically wakes up to receive new messages addressed to it. Sensing tasks are distributed to all nodes, thus energy consumption variance among nodes is kept small.

Bounded Sufficient Phase and Worst-Case x Stealth Distance. We define the x *stealth distance* as the distance a moving object travels on x-axis before it is detected. A *handoff* is defined as the process when active lines advance to their new positions, all nodes covering the new lines wake up, and those nodes covering old lines only go to sleep.

Theorem 1. *In the line wave protocol, the sufficient phase of any moving object is bounded by* $2P$*, where* P *is the wave sensing period. In other words, the moving object can always be detected in* $2P$*.*

Proof: Consider the handoff process of an active line in the line wave protocol. Suppose this line moves from left to right. We denote the old active line as ol, and denote the new active line as nl. Note that the distance between ol and nl is less than $2R$. We first prove that there is no sensing hole in the union of ol's hot region and nl's hot region.

We use contradiction in the proof. Suppose there is a sensing hole H in the sensing range union. Consider a point $p \in H$. When all nodes on the field wake up, the field can be completely covered. Thus, there must exist a sensor s that can cover p when it wakes up. Denote the circle of s's sensing range as C. We know that C either intersects ol or nl or both. If not, there could be several cases.

– All points in C are between ol and nl, as shown in Fig. 2(a). Consider the diameter of C on x-axis. Because the diameter has a length of $2R$, while the distance between

ol and nl is less than $2R$, the diameter must intersect at least one of these two lines. Then s must be active. This contradicts the assumption that p is not covered.

- Part of points in C are between ol and nl, and part of points in C are on the left of ol, or on the right of nl. Then we choose a point p between ol and nl, and a point on the left of ol, as shown in Fig. 2(b), or a point on the right of nl, as shown in Fig. 2(c). Denote this point as $p1$. We draw a line to connect p and $p1$, then this line must intersect either ol or nl. Thus, s should be active. This contradicts the assumption that p is not covered.
- All points in C are totally on the left of ol, or on the right of nl. This is impossible, because it contradicts the assumption that p is covered by s.

Therefore, there is no sensing hole in the hot regions of ol and nl.

We next prove an object can be detected in $2P$. As shown in Fig. 3, in a handoff process, the field is divided by the four active lines into five regions, denoted as A, B, C, D, and E, respectively. Consider the initial position $O1$ of the moving object.

- If $O1 \in A \cup E$, after one scanning period P, $O1 \in C$. After another period P, $C = \phi$. This means that the trajectory of this object must have intersected one of the active lines, thus has been detected.
- If $O1 \in B \cup D$, it is covered by the sensing ranges of active sensors, thus has already been detected.
- If $O1 \in C$, then after one scanning period P, $C = \phi$. This means that the trajectory of this object has encountered one of the active lines at least once, thus has been detected.

In summary, the object can always be detected in $2P$. □

Lemma 1. *The worst-case x stealth distance is less than $2vP$. If the object moves along a straight line with an even speed v, the worst-case x stealth distance is less than L.*

Proof: According to Theorem 1, the object is detected in $2P$ time. The distance that the object travels in $2P$ is $2vP$.

Suppose that the object travels along a straight line, and it takes $2P$ to detect this object. In the first P, when the object is behind one of the active lines and is chasing that line, it can travel at most $\frac{L}{2}$ on x-axis without being detected. In the second P, the object is between the two active lines, the maximum x distance it can travel is $\frac{L}{2}$. Therefore, the object can travel at most L on x-axis before being detected. □

3.2 Stripe Wave Protocol Design

One restriction of the line wave protocol is the precision requirement on node coordinates. To relax this constraint, we design a stripe wave protocol. In this protocol, stripes, instead of lines, are covered by active sensors, as shown in Fig. 4. When the stripe width is larger than the required coordinate precision, object detection quality can be achieved.

In the stripe wave protocol, nodes wake up if their sensing ranges intersect active stripes. The width of active stripes is twice of their advancing distance. In this way, there is an overlap between the old stripe and the new stripe. All the other procedures remain the same as those of the line wave protocol.

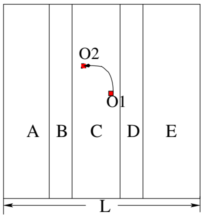

Fig. 3. The object is detected in the line wave protocol

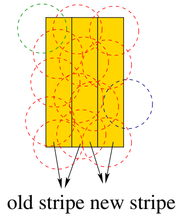

Fig. 4. The sensing stripe handoff in the stripe wave protocol

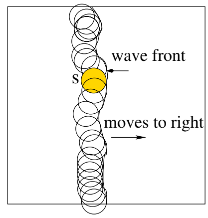

Fig. 5. The wave front moves in the distributed wave protocol

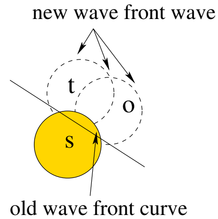

Fig. 6. An active sensor activates a set of nodes to cover its wave front curve

Sufficient Phase and Worst-Case x Stealth Distance of Stripe Wave Protocols. If one active stripe stays in a place for the same amount of time, and advances the same distance in the same direction as the active lines of the line wave protocol. Then for any point p on the field, if p is covered in the line protocol, it is also covered in the stripe protocol. From Theorem 1 and Lemma 1, we can have the following two corollaries.

Corollary 1. *In the stripe wave protocol, the sufficient phase of a moving object is at most* $2P$*, where* P *is the wave sensing period. In other words, the moving object can always be detected in a duration of* $2P$*.*

Corollary 2. *The worst-case* x *stealth distance is less than* $2vP$*. If the object moves along a straight line with an even speed, then the worst-case* x *stealth distance is less than* L*.*

3.3 Distributed Wave Protocol

As described above, the line wave and stripe wave protocols require global clock synchronization. To relax such requirement, we design a distributed wave protocol that can be implemented locally on each individual node, and does not need timer synchronization among nodes.

Hot Regions and Wave Fronts. In this distributed wave protocol, there are two continuous active curves with two ends on two opposite borders of the field. These two curves scan the sensing field periodically, so that every point can be covered at least once during one wave sensing period. A set of sensors wake up to cover these curves. We define the *hot region* of an active curve as the union of sensing ranges of active sensors covering this curve, and define the *wave front* of the curve as the boundary of its hot region in its moving direction. Fig. 5 illustrates the wave front of a hot region moving to the right. Since the active curve is continuous, the wave front is continuous as well. For an active curve scanning the field from left to right, its wave front also moves from left to right.

Active Curves Move Forward. Here we describe how an active curve moves forward in our distributed wave protocol. Consider an active sensor s that has part of its sensing circle on the wave front of the active curve. As shown in Fig. 6, we define the wave front curve of s as the part of its sensing circle on the wave front. Before s goes to sleep, it finds all nodes whose sensing ranges intersect its wave front curve to wake up. After those sensors become active, part of their sensing circles become part of the new wave front. For example, in Fig. 6, before s goes to sleep, it finds node t and node o to wake up because the sensing ranges of t and o intersect the wave front curve of s. In this way, the wave front of an active curve always moves forward, eventually it reaches the center vertical line of the field. The same process repeats afterwards.

Note that a sensing hole is a set of continuous points on the field that have not been covered in one scanning period. We have the following theorem.

Theorem 2. *In the distributed wave protocol, the wave front of an active curve can scan the whole sensing field in an finite time without leaving any sensing hole.*

Proof: Consider an active sensor s that has part of its sensing circle on the wave front. We claim that s can always find a set of sensors that have not waked up in current scanning period to cover s's wave front curve.

Let $P(t)$ be the set of points on the field that have been sensed at time t in current scanning period, then we have $P(t) \subset P(t + \Delta t)$, where Δt is a time increment. In other words, the wave front always moves forward and does not go back. For any point p on the field, $p \in P(t) \Rightarrow p \in P(t + \Delta t)$. This implies that if a point $p \in P(t)$, then p is behind the wave front at time $t + \Delta t$. Therefore, the sensors that had already waked up and gone back to sleep in the past cannot cover points on the current wave front. Since any point on the field is within the sensing range of some sensor, there must exist a set of sensors that can cover s's wave front. Thus, we can find sensors that had not waked up to cover s's front wave curve at time $t + \Delta t$. On the other hand, according to the design of this distributed wave protocol, the wave front is continuous with two ends on the opposite borders of the field. Therefore, no sensing hole will be created in this distributed protocol. □

Lemma 2. *In one scanning period, every node on the field wakes up exactly once, and consumes the same amount of energy given that they stay awake for the same amount of time.*

Proof: We assume that no two sensor nodes are located at the same geographical coordinates. We only consider one of the active curves, since the proof can be applied to the other curve due to the symmetry. When a node goes to sleep, it always activates those nodes ahead of the wave front to cover its wave front curve. We use induction to prove that the nodes behind the wave have already waked up once.

– Base. At system start-up time, the active curve is on a side border of the square. Only a set of nodes wake up to cover this curve, and all other nodes have not waked up yet.
– Induction step. Suppose at time t, all nodes behind the wave front have waked up once and only once. Consider the next earliest moment that one active node on the wave front goes to sleep. It activates all nodes that can partly cover its wave front curve. Because these newly-activated sensors are ahead of the wave front, they were in sleeping mode before time t, and have just waked up at t.

On the other hand, if a node has not waked up yet, its sensing range must intersect the wave front curve of some node m at some moment t', where t' is less than the scanning period. Therefore, it will be activated by node m at some moment. □

We directly obtain the following conclusion from Lemma 2.

Corollary 3. *The scanning period of this distributed wave protocol is less than $wt \cdot n$, where wt is the active duration of nodes in one scanning period and n is the total number of nodes on the sensing field.*

3.4 Partially-Covered Sensing Field

In the partially-covered sensing field, only if the object moves in the covered region, can it be detected in a bounded time with a bounded worst-case stealth distance before detection by using three sensing protocols proposed above.

4 Modeling and Analysis of Wave Sensing Scheduling Scheme

From the earlier protocol design, we know that the scanning period P of the line wave and stripe wave protocols is independent of sensor locations on the field. However, in the distributed wave protocol, the scanning period P is decided by the sensor locations, not controlled by the protocol itself. In this section, we first establish a model for the line wave and stripe wave protocols, then we analyze average-case object detection quality and energy consumption properties of the wave schedules under this model.

In the model, nodes are assumed to be densely deployed on a square field so that the field can be completely covered when all nodes wake up. The field is divided into many identical stripes (in the one-dimensional (*1-d*) wave schedule) or squares (in the two-dimensional (*2-d*) wave schedule), in each of which there are active lines periodically moving through with a constant speed, as shown in Fig. 7 and Fig. 8. The parameters of the model are listed in Fig. 11.

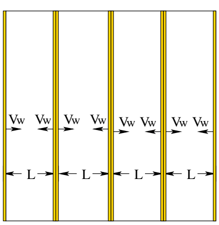

Fig. 7. *1-d* wave schedule illustration

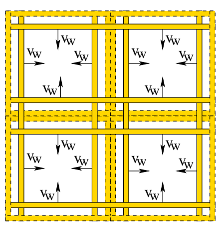

Fig. 8. *2-d* wave schedule illustration

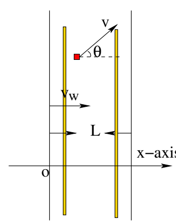

Fig. 9. DP and ASD analysis of the *1-d* wave schedule

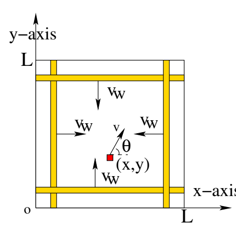

Fig. 10. DP and ASD analysis of the *2-d* wave schedule

In the *1-d* wave schedule, the sensing field is divided into multiple parallel vertical stripes with widths of L, as shown in Fig. 7. Two active lines start from the two borders

parameter	meaning
d	density of sensors
R	sensing radius of a sensor
v	speed of a moving object
P	scanning period of the scheme
f	active ratio of sensors in P
v_w	wave line scanning speed
t_a	observation duration
wt	line (curve) settling time
L	side length of a stripe or a square

Fig. 11. Model parameters of the wave protocols

	DP	ASD
$d \uparrow$	$\rightarrow$	$\rightarrow$
$R \uparrow$	$\rightarrow$	$\rightarrow$
$v \uparrow$	$\uparrow$	$\uparrow$
$t_a \uparrow$	$\uparrow$	$\rightarrow$
$wt \uparrow$	$\downarrow$	$\uparrow$

Fig. 12. DP and ASD change when parameters increase in the model

of each stripe moving towards the stripe center with a constant speed v_w. Once they reach the center, the process starts over again. In the *2-d* wave schedule, the sensing field is divided into multiple equally-sized squares with side lengths of L, as shown in Fig. 8. Four active lines start from the four borders of the square moving towards the square center. Once they reach the center, they return to the borders, and the process repeats. Note that the width of hot regions is negligible considering the vastness of the stripes and the squares.

From the model, we know that $P = \frac{L}{2v_w}$, and $f = \frac{4R}{L}$.

4.1 *1-d* Wave Schedule Analysis

Now we mathematically analyze the DP and ASD of the *1-d* wave schedule under our model.

Detection Probability. Consider the sensing stripe where the object is located. We view this stripe as a Euclidean coordinate space with an origin on its left border, as shown in Fig. 9. Note that L is negligible compared to the height of the stripe. Two active lines move from the two borders of the stripe towards the center with a speed of v_w. We define $mod(z_1, z_2)$ as the remainder of z_1 divided by z_2 for any two variables z_1 and z_2.

Suppose at system startup time 0, the object is located at (x, y), and the two active lines are on the two borders of the stripe. Let t be the time when we start observation, where $0 \leq t \leq 2P$. At time t, the x-coordinates of the two active lines are $mod(v_w t, \frac{L}{2})$ and $L - mod(v_w t, \frac{L}{2})$. Since the object can move in any direction, we denote the angle between its moving direction and the x-axis as θ. Then the x-coordinate of the object is $x + vt\cos\theta$ at time t. If the object and one of the active lines meet at time t', then we know $x + vt'\cos\theta = mod(v_w t', \frac{L}{2})$, or $x + vt'\cos\theta = L - mod(v_w t', \frac{L}{2})$.

Define the meeting function $t_i(x, \theta)$ as the time it takes for the ith wave line to meet the object from the system startup time, where $i = 1, 2$. We know whether the object is detected depends on the observation duration t_a. If $t_a < t_1(x, \theta)$ and $t_a < t_2(x, \theta)$, the object cannot be detected. Otherwise, it can be detected.

Suppose after t_m time, the moving object is detected. Denote t_{m1} and t_{m2} as the time for the object to meet the left active line and the right active line, respectively. Then we have $x + vt_{m1}\cos\theta = mod(v_w t_{m1}, \frac{L}{2})$ and $x + vt_{m2}\cos\theta = L - mod(v_w t_{m2}, \frac{L}{2})$. Thus, $t_m(x, \theta, t) = min(t_{m1}(x, \theta), t_{m2}(x, \theta)) - t$.

We define a new boolean detecting function $D(\theta, x, t)$ as follows:

$$D(\theta, x, t) = \begin{cases} 1, \text{ when } t_a \geq t_m(x, \theta, t). \\ 0, \text{ when } t_a < t_m(x, \theta, t). \end{cases}$$

To get the detection probability DP, we integrate $D(\theta, x, t)$ over t, x, and θ, respectively. Therefore, we can get the following theorem.

Theorem 3. *In the* 1-d *wave schedule,* $DP = \frac{\int_0^{2P} \mathrm{d}t \int_0^L \mathrm{d}x \int_0^{2\pi} D(\theta,x,t)\mathrm{d}\theta}{4\pi PL}$.

Average Stealth Distance. Consider the distance dis this object travels in the observation duration t_a, we have $dis = vt_m(x, \theta, t)$. To derive the average stealth distance, we integrate this dis over the ranges of the three variables θ, x, and t, respectively. Then we have the following lemma.

Lemma 3. *In the* 1-d *wave schedule,* $ASD = \frac{\int_0^{2P} \mathrm{d}t \int_0^L \mathrm{d}x \int_0^{2\pi} vt_m(x,\theta,t)\mathrm{d}\theta}{4\pi PL}$.

Sufficient Phase and Worst-case x Stealth Distance. From the analyses of the line wave and stripe wave protocols, we have the following corollaries.

Corollary 4. *The sufficient phase in* 1-d *wave schedule is less than* $2P$.

Corollary 5. *In the* 1-d *wave schedule, the worst-case x stealth distance is upper bounded by* $min(2vP, L)$.

4.2 *2-d* Wave Schedule Analysis

In the *2-d* wave schedule, the sensing field is divided into repetitive grid squares so that an object can be detected more quickly.

Detection Probability. Suppose we start our observation at time t, where $0 \leq t \leq 2P$. We consider the square where the moving object is located, and view it as a Euclidean coordinate space with an origin on its left bottom corner. Assume the object is located at (x, y) with a moving speed of v, where $0 \leq x \leq L$, $0 \leq y \leq L$. Denote the angle between its moving direction and the x-axis as θ.

At time t', the location functions of the four active lines are: $x(t') = mod(v_w t', \frac{L}{2})$; $x(t') = L - mod(v_w t', \frac{L}{2})$; $y(t') = mod(v_w t', \frac{L}{2})$; and $y(t') = L - mod(v_m t', \frac{L}{2})$. The coordinates of the object are: $x + vt'\cos\theta, y + vt'\sin\theta$. If the object is not detected, it must be inside the square whose borders are the four active lines, as shown in Fig. 10. Thus, we have $mod(v_w t', \frac{L}{2}) < x + vt'\cos\theta < L - mod(v_w t', \frac{L}{2})$, and $mod(v_w t', \frac{L}{2}) < y + vt'\sin\theta < L - mod(v_w t', \frac{L}{2})$. Otherwise, if these conditions are not satisfied, the object is detected.

Denote t_{m1}, t_{m2}, t_{m3}, and t_{m4} as the time when the object meets the four active lines respectively, then we have: $x + vt_{m1}\cos\theta = mod(v_w t_{m1}, \frac{L}{2})$; $x + vt_{m2}\cos\theta = L - mod(v_w t_{m2}, \frac{L}{2})$; $y + vt_{m3}\sin\theta = mod(v_w t_{m3}, \frac{L}{2})$; and $y + vt_{m4}\sin\theta = L - mod(v_w t_{m4}, \frac{L}{2})$. The time it takes to detect the object when starting observation from t can be calculated as: $t_m(x, y, \theta, t) = min(t_{m1}, t_{m2}, t_{m3}, t_{m4}) - t$.

We define a detection boolean function

$$D(x, y, \theta, t) = \begin{cases} 1, & \text{if } t_a \geq t_m(x, y, \theta, t). \\ 0, & \text{if } t_a < t_m(x, y, \theta, t). \end{cases}$$

Similar to the *1-d* wave analysis, we can get the following theorem immediately.

Theorem 4. *In the* 2-d *wave schedule,* $DP = \frac{\int_0^{2P} \mathrm{d}t \int_0^{2\pi} \mathrm{d}\theta \int_0^L \mathrm{d}x \int_0^L D(x,y,\theta,t) \mathrm{d}y}{4\pi P L^2}$.

Average Stealth Distance. The average detecting time is $\overline{DT}(x, y, \theta, t) = \frac{\int_0^{2P} \mathrm{d}t \int_0^{2\pi} \mathrm{d}\theta \int_0^L \mathrm{d}x \int_0^L t_m(x,y,\theta,t) \mathrm{d}y}{4\pi P L^2}$. Therefore, we have the following lemma.

Lemma 4. *In the* 2-d *wave schedule,* $ASD = \frac{\int_0^{2P} \mathrm{d}t \int_0^{2\pi} \mathrm{d}\theta \int_0^L \mathrm{d}x \int_0^L vt_m(x,y,\theta,t) \mathrm{d}y}{4\pi P L^2}$.

Sufficient Phase and Worst-Case Stealth Distance. Similar to the analyses in the line wave and stripe wave protocols, we have the following bounds for sufficient phase and worst-case stealth distance.

Lemma 5. *In the* 2-d *wave schedule, the sufficient phase of an object is not greater than* $2P$*. In other words, when* $t_a > 2P$*, the object is detected with certainty.*

Proof: Consider the initial location $O1$ of the object when we start our observation.

We define interior squares as the shrinking squares with the active lines as their borders.

- If $O1$ is inside an interior square, the object will meet one of the active lines after a period P, thus will be detected.
- Suppose $O1$ is outside all interior squares. After one period P, if it meets the active lines, it is detected. If it is not detected in one P, then it enters one interior square. After another P, this object will be detected.

Therefore, its sufficient phase is not greater than $2P$. □

Corollary 6. *In the* 2-d *wave schedule, the worst-case stealth distance is less than* $2vP$*. If the object moves along a straight line with a constant speed, then its worst-case stealth distance is less than* $\sqrt{2}L$*.*

Proof: The first part is a direct conclusion from Lemma 5. Suppose the object moves a time of $2P$ before being detected. In the first P, the object can move a distance of at most $\frac{\sqrt{2}L}{2}$, which is the half of the diagonal length of the square. In the second P, the object can move at most $\frac{\sqrt{2}L}{2}$ as well. Therefore, the object can move at most $\sqrt{2}L$. □

4.3 Node Remaining Energy and System Lifetime

Let T be the continuous working time of a node, and all nodes have the same T. Then in the wave schedules, in the ith period, nodes have remaining energy in the range $[T - ifP, T - (i-1)fP]$ for $1 \leq i \leq \frac{T}{fP}$. A node will last for $\frac{T}{fP}$ periods, thus its working time is $\frac{T}{fP} \cdot P = \frac{T}{f}$. This implies that the system lifetime is $LT = \frac{T}{f}$.

5 Evaluation of Wave Protocols

We conduct extensive simulation experiments to verify our analyses and to evaluate the wave protocols. We assess the average-case object detection quality based on the simulation results of DP and ASD.

In our experiments, we generate a 200×200 grid field, and randomly place $d \times 40,000$ sensors on it. One constraint on these sensors is that when all of them are active, their sensing ranges should be able to cover the whole sensing field. A small object moves along a straight line with a constant speed v. We generate two active sensing lines or stripes at the two borders of the field moving towards the center periodically. We run each simulation for hundreds of times. We use the ratio of times of detection over the number of experiments to estimate DP, and use the average non-detecting distance to estimate ASD. Since we have given upper bounds on the SP and the WSD in the protocol design part, we do not evaluate them in our experiments. Effects of system parameters on DP and ASD of the line wave and stripe wave protocols are listed in Fig. 12.

5.1 Comparison of the Three Wave Protocols

Different from the line wave and stripe wave protocols, the wave sensing period of the distributed wave protocol depends on geographical locations of the nodes. We compare the wave sensing period of these three protocols under the following parameter setting: $d = 0.3, R = 1.5, wt = 0.5$, and $v_w = 5.4$. We find that $P_{line} = 74.8$, $P_{stripe} = 75.3$, and $P_{dist} = 71.5$. This means the distributed wave protocol scans the field faster than the other two protocols at the cost of extra energy consumption.

To compare the DP, ASD, and energy consumption of different wave protocols, we use the same set of parameters except P for one simulation scenario. In the line wave and stripe wave protocols, ad is slightly less than $2R$. Note that $L = 200$, and $P = \frac{2L}{v_w}$.

DP and ASD Results. In all our experiments on DP, we restrict that $t_a < P$ to make sure that DP varies between 0 and 100%. Figures 13 and 14 demonstrate that all three protocols have close DP and ASD results. However, the distributed wave protocol performs slightly different from the other two protocols, it has a higher DP and a lower ASD. When either v or t_a increases, DP increases too, which is shown in Fig. 13(a). Fig. 13(b) shows that a larger wt incurs a smaller DP. On the other hand, a larger v incurs a larger ASD, as shown in Fig. 14(a). Interestingly, the ASD increases linearly when node settling time wt increases, as we can observe from Fig. 14(b). This is because for a larger wt, it takes longer for an active line or stripe to scan the field than a smaller wt, thus the object can travel a longer distance.

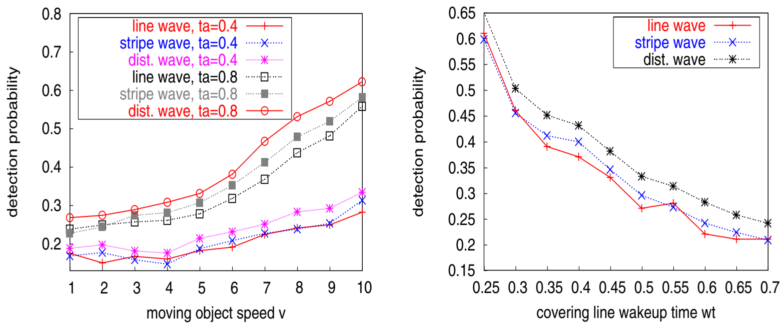

(a) DP when varying v. $d = 0.3, R = 1.5, wt = 0.05, v_w = 50$.

(b) DP when varying wt, $d = 0.3, R = 1.5, v = 1, t_a = 8, v_w = 5$.

Fig. 13. DP of the wave protocols when varying different parameters

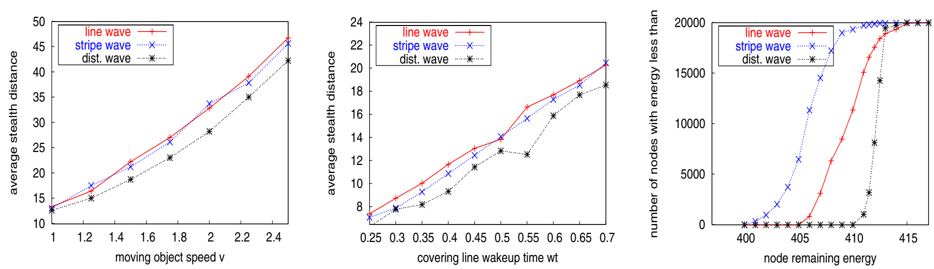

(a) ASD when varying v. $d = 0.3, R = 1.5, wt = 0.5, v_w = 50$.

(b) ASD when varying wt, $d = 0.3, R = 1.5, v = 1, v_w = 5$.

(c) Node energy cumulative distribution. $d = 1, R = 1, wt = 1$.

Fig. 14. ASD and node energy distribution when varying different parameters

Node Energy Distribution Result. All nodes have the same energy E at the beginning, and node energy consumption rate is $er = C \cdot R^3 \cdot \frac{2R}{v_w} / \frac{L}{2v_w} = \frac{4CR^4}{L}$, where C is a constant being dependent on hardware design of the sensor nodes. We set $C = 0.00625$. We draw the node energy cumulative distribution in Fig. 14(c) to further show energy variance among nodes. For any curve point in this figure, its x value represents the node remaining energy, and its y value represents the number of nodes with energy less than the value specified by the x-axis. We observe that the remaining energy of most nodes is around the average node energy of the network. On the other hand, the node energy distribution of the distributed wave protocol has a narrower range than those of the other two wave protocols.

5.2 Comparison of Line Wave, Random, and Synchronized Schedules

In [12], we have formally studied the random sensing schedule and the synchronized sensing schedule. In Figures 15 and 16, we compare the analytical DP and ASD results

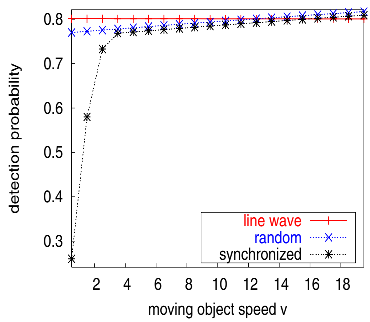

Fig. 15. DP when varying v. $d = 1, R = 0.75, t_a = 0.4, wt = 0.01, v_w = 2$

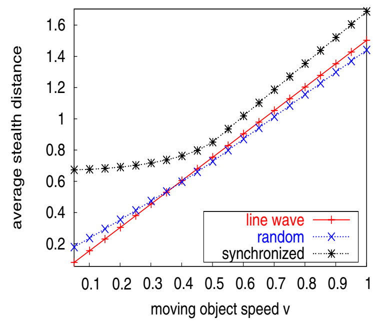

Fig. 16. ASD when varying v. $d = 1, R = 0.75, wt = 0.01, v_w = 2$

of the line wave schedule, the random schedule, and the synchronized schedule, respectively, when varying v and fixing all other parameters. We observe that, with a small v, the line wave schedule and the random schedule have a larger DP than the synchronized sensing schedule; however, as v increases, the synchronized schedule begins to catch up the line wave schedule, and eventually outperforms it. Similarly, the line wave schedule has a smaller ASD for small v. When v increases, the ASD of the line wave schedule exceeds that of the random sensing schedule, and the synchronized schedule has a larger ASD than the other two schedules.

6 Related Work

Extensive work has been conducted on object-tracking with different approaches: system design and deployment [6, 13], design of high tracking-precision protocols [2], design of energy-efficient tracking protocols [11], and design of protocols to exploit node collaborations [3, 7, 9, 10, 17]. In [11], Pattem *et al.* proposed duty-cycled activation and selective activation algorithms to balance tracking errors and energy expenditure. Gui *et al.* [5] studied the quality of surveillance of several sensing scheduling protocols. [13] is a work covering design of hardware, networking architecture, and control and management of remote data access. Increasing the degree of sensing coverage can usually improve object detection and tracking quality. Along this direction, many power-efficient sensing coverage maintenance protocols [1, 4, 14, 15] have been proposed in the literature. Yan *et al.* [15] presented an energy-efficient random reference point sensing protocol to achieve a targeted coverage degree. In [16], Zhang and Hou studied the system lifetime of a k-covered sensor network, and proved that it is upper bounded by k times node continuous working time.

7 Conclusion

In this paper, we designed three wave sensing scheduling protocols to provide bounded worst-case object detection quality for many surveillance applications. One of the protocols is distributed and can be implemented locally on each individual node. In these protocols, sensing field is scanned by a set of connected active sensors periodically. In addition, we characterized the interactions among network parameters, and analyzed average-case object detection quality and energy consumption of the protocols. We proved the correctness of the proposed protocols and evaluated their performances through extensive simulations.

Acknowledgment

We are grateful to the anonymous reviewers for their constructive comments and suggestions. We also acknowledge William L. Bynum for reading an earlier version of the paper. This work is partially supported by the U.S. National Science Foundation under grants CNS-0098055, CCF-0129883, and CNS-0405909.

References

1. Z. Abrams, A. Goel, and S. Plotkin. Set k-Cover algorithms for energy efficient monitoring in wireless sensor networks. In *Proceedings of IPSN'04*.
2. J. Aslam, Z. Butler, F. Constantin, V. Crespi, G. Cybenko, and D. Rus. Tracking a moving object with a binary sensor network. In *Proceedings of ACM SenSys'03*.
3. R. Brooks, P. Ramanathan, and A. Sayeed. Distributed target classification and tracking in sensor networks. In *International Journal of High Performance Computer Applications, special issue on Sensor Networks*, 16(3), 2002.
4. P. B. Godfrey and D. Ratajczak. Naps: scalable, robust topology management in wireless ad hoc networks. In *Proceedings of IPSN'04*.
5. C. Gui and P. Mohapatra. Power conservation and quality of surveillance in target tracking sensor networks. In *Proceedings of ACM MobiCom'04*.
6. T. He, S. Krishnamurthy, J. Stankovic, T. Abdelzaher, L. Luo, R. Stoleru, T. Yan, L. Gu, J. Hui, and B. Krogh. Energy-efficient surveillance system using wireless sensor networks. In *Proceedings of ACM/USENIX MobiSys'04*.
7. D. Li, K. Wong, Y. Hu, and A. Sayeed. Detection, classification and tracking of targets in distributed sensor networks. In *IEEE Signal Processing Magazine*, pages 17–29, March 2002.
8. Q. Li and D. Rus. Global clock synchronization in sensor networks. In *Proceedings of IEEE INFOCOM'04*.
9. J. Liu, M. Chu, J. Liu, J. Reich, and F. Zhao. Distributed state representation for tracking problems in sensor networks. In *Proceedings of IPSN'04*.
10. J. Liu, J. Liu, J. Reich, P. Cheung, and F. Zhao. Distributed group management for track initiation and maintenance in target localization applications. In *Proceedings of IPSN'03*.
11. S. Pattem, S. Poduri, and B. Krishnamachari. Energy-quality tradeoffs for target tracking in wireless sensor networks. In *Proceedings of IPSN'03*.
12. S. Ren, Q. Li, H. Wang, X. Chen, and X. Zhang. Analyzing object detection quality under probabilistic coverage in sensor networks. In *Proceedings of IWQoS'05*.
13. R. Szewczyk, A. Mainwaring, J. Polastre, and D. Culler. An analysis of a large scale habitat monitoring application. In *Proceedings of ACM SenSys'04*.
14. X. Wang, G. Xing, Y. Zhang, C. Lu, R. Pless, and C. Gill. Integrated coverage and connectivity configuration in wireless sensor networks. In *Proceedings of ACM SenSys'03*.

15. T. Yan, T. He, and J. Stankovic. Differentiated surveillance for sensor networks. In *Proceedings of ACM SenSys'03*.
16. H. Zhang and J. Hou. On deriving the upper bound of α-lifetime for large sensor networks. In *Proceedings of ACM MobiHoc'04*.
17. W. Zhang and G. Cao. Optimizing tree reconfiguration for mobile target tracking in sensor networks. In *Proceedings of IEEE INFOCOM'04*.